

## Directional Correlation of Fission Fragments and Prompt Gamma Rays Associated With Thermal Neutron Fission\*†

MARVIN M. HOFFMAN

*Los Alamos Scientific Laboratory, Los Alamos, New Mexico*

(Received 29 April 1963; revised manuscript received 6 November 1963)

Prompt fission  $\gamma$ -ray intensity as a function of the angle from the fragment direction has been measured for the thermal neutron fission of  $U^{235}$ ,  $U^{238}$ , and  $Pu^{239}$ . For each of these three nuclides, the fission  $\gamma$  rays were found to be emitted preferentially in the direction of fragment motion by as much as 15%. It was found that the experimental data were best fitted by assuming that  $\gamma$  rays emitted by fission fragments have two components with different angular distributions. One component, accounting for about 85% of the  $\gamma$  rays, was isotropic about the fission fragment direction. The remaining 15% had the angular distribution of  $\gamma$  rays from quadrupole transitions of nuclei having approximately 7 units of angular momentum distributed in, or near, a plane perpendicular to the direction of fragment motion. A calculation of the torque resulting from electrostatic forces between the fission fragments is discussed. Results of this calculation indicate that these electrostatic forces could give rise to the fragment rotations indicated by the  $\gamma$ -ray measurements.

### INTRODUCTION

MEASUREMENTS of the anisotropy  $A$  of prompt  $\gamma$  rays from thermal neutron fission have given values as large as  $A=0.30$ ,<sup>1,2</sup> where  $A$  is taken as the ratio of  $[I(0)-I(90)]/I(90)$ . Here  $I(\theta)$  refers to the relative number of  $\gamma$  rays observed per unit solid angle at the angle  $\theta$  from the direction of motion of the fission fragment. It is significant that fission neutrons, which can easily be mistakenly recorded as  $\gamma$  rays, might account for part or all of the observed anisotropy. With this in mind, an experiment has been performed to measure  $I(\theta)$  for  $\gamma$  rays of energy greater than 250 keV emitted in conjunction with a thermal neutron fission event. In this experiment, the probability of mistaking neutrons for  $\gamma$  rays has been greatly reduced by employing a fast coincidence circuit which rejected most fission neutrons as a result of their delayed arrival at the  $\gamma$  counters. These measurements were carried out using a thermal column of the Los Alamos water boiler, and fissionable foils of  $Pu^{239}$ ,  $U^{235}$ , and  $U^{238}$ . A 70-cm path length from the fission source to the  $\gamma$  counter gave rise to an adequate delay in the neutron arrival. The relative  $\gamma$ -ray intensity has been measured at several angles from the fragment direction in the interval  $0 < \theta < \pi/2$ .

The correlation function observed in this interval will have forward-backward, in addition to right-left symmetry, because of the inability to determine from which fragment the  $\gamma$  ray had originated, and because the fission counter could accept either the heavy or light fragment. Because of these two properties of the experi-

ment, all reference to the measured  $\gamma$ -ray intensity  $I(\theta)$  is actually the sum of  $I(\theta)$  from the heavy fragment plus  $I(\pi+\theta)$  from the light, combined with equal parts of  $I(\theta)$  from the light fragment plus  $I(\pi+\theta)$  from the heavy. Some data were taken with the fission counter biased to accept only heavy fragments or only light fragments, but not both. No discernible difference was observed in the  $I(\theta)$  measured under these two conditions which indicates that  $I(\theta)_h + I(\pi+\theta)_l = I(\theta)_l + I(\pi+\theta)_h$  within the accuracy of the experiment. The observed correlation of  $\gamma$ -ray intensity with the direction of fission fragment motion leads to the investigation of a correlation of the fission fragment angular momentum and its direction of motion.

The brief consideration given to fission fragment angular momentum in this paper deals only with the obvious effect of electrostatic forces between nuclear matter in nonspherical configurations. An attempt has been made to treat this question in a systematic fashion although the treatment is neither complete nor rigorous at several points.

### EXPERIMENTAL EQUIPMENT AND PROCEDURES

Placement of the fission counter and the  $\gamma$ -ray counters together with their neutron and  $\gamma$  shielding is depicted in Fig. 1. The slow neutron beam was trapped in a boron-loaded paraffin catcher as close to the fission counter as possible. Uncaught neutrons were troublesome from the standpoint of personnel safety, and they hampered the experiment by producing a high level of 25-min  $I^{28}$  activity in the NaI(Tl) crystals, which contributed to the accidental coincidence counting rate. In addition to the beam catcher, a  $\frac{1}{4}$ -in.-thick shield of natural lithium metal covered the crystals and extended back along the photomultiplier tubes to further reduce  $\gamma$  rays from thermal neutron capture in the sodium iodide crystals. Lead was placed around the  $\gamma$  counters in sufficient thickness to attenuate the extraneous  $\gamma$  intensity to a level well below the irreducible portion

\* This work performed under the auspices of the U. S. Atomic Energy Commission at Los Alamos Scientific Laboratory, University of California, Los Alamos, New Mexico.

† Some of the material in this paper was presented at the "Discussion on Nuclear Chemistry (Fission and Other Low Energy Nuclear Processes)," Oxford, England, 18-20 September 1962.

<sup>1</sup> *Progress in Nuclear Physics*, edited by O. R. Frisch (Pergamon Press, Ltd., London, 1952), p. 152.

<sup>2</sup> C. C. Trail and C. M. Huddleston, *Bull. Am. Phys. Soc.* **2**, 70 (1957).

which was scattered into the counters from the immediate vicinity of the fission source.

### Fission Source and Counter

The fission sources for this experiment were comprised of approximately  $1.1 \text{ mg/cm}^2$  of fissionable material in the form of an oxide evaporated onto a circular aluminum disk 3 cm in diameter. The  $\text{Pu}^{239}$  fission source was contaminated with 5.3% of  $\text{Pu}^{240}$  while the abundance of undesirable isotopes in  $\text{U}^{235}$  and  $\text{U}^{238}$  sources was less than 0.3%. The aluminum disk was sufficiently thick,  $34 \text{ mg/cm}^2$ , to stop all fragments moving into the  $2\pi$  solid angle covered by the backing. The time required for a fission fragment moving through aluminum to come to rest is between  $10^{-12}$  and  $10^{-13}$  sec, so it can reasonably be assumed that prompt  $\gamma$ -ray emission by the fragment nucleus will be rapid compared to the fragment stopping time and, therefore, unaffected by the presence of the backing. One can test this assumption using the relativistic effect on the flux of  $\gamma$  rays emitted by moving fission fragments since this will produce an increase in the flux along the line of fragment motion over the flux at right angles to the fragment motion of about 0.3%, when measured in the laboratory system. This value is based on the premise that heavy and light fragments emit the same number of  $\gamma$  rays, and that equal numbers move each way along the selected path. If, on the other hand, all fission fragments moving in one direction are stopped prior to the emission of  $\gamma$  rays while those moving in the opposite direction are not, the  $\gamma$ -ray flux ratio of  $I(0)/I(90)$  in the laboratory system would change by 4%. The test was carried out by measuring  $I(0)/I(90)$  using fission sources on first a thick, and then, a thin backing. The results of this experiment indicated that whether or not the fragments were stopped in an aluminum backing had no effect on the ratio of  $\gamma$ -ray

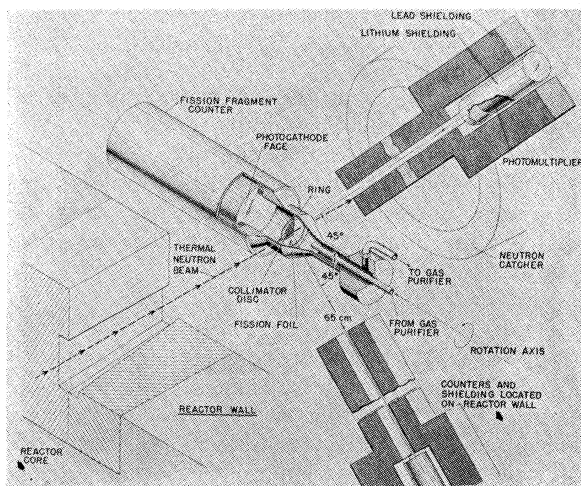


FIG. 1. Counter configuration used to measure fission fragment  $\gamma$ -ray correlation.

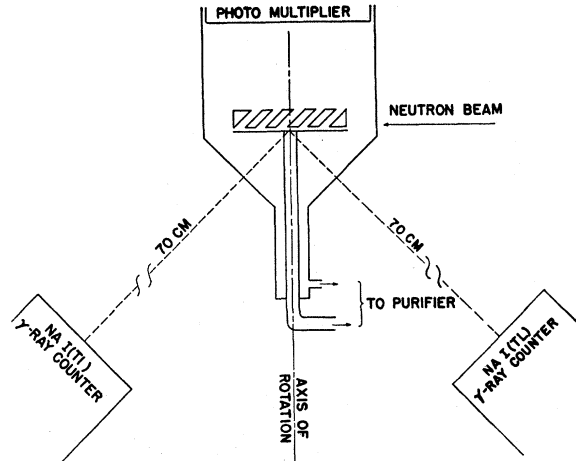


FIG. 2. Schematic diagram of fission fragment counter.

fluxes measured at 0 and  $90^\circ$  in the laboratory system. It should be mentioned, however, that because of the statistics of the experimental data and the magnitude of the possible effect, there was a 20% chance that the effect would be unobserved even though it did exist.

All angular correlation data presented were taken with the fissionable material sandwiched between a heavy aluminum backing and a fragment collimator disk. This assembly was held together and positioned inside the sensitive volume of a gas scintillator-type fission fragment counter by an aluminum retainer ring. The fragment collimator was a 1.5-mm-thick, 30-mm-diam aluminum disk perforated by 362 parallel holes at  $45^\circ$  from the normal to the surface of the disk. The angle between the axis of the fragment collimating aperture and a fixed line to the  $\gamma$ -ray counter was then varied between 0 and  $90^\circ$  by rotating the entire fragment counter about its axis which passed through the center of the collimating disk and was perpendicular to its surface as shown in Fig. 2. The solid angle for transmission through this collimator changes appreciably with position at the entrance aperture; therefore, the collimator was analyzed by a machine calculation. This calculation gave a transmission through the collimating holes of 0.013, and indicated that the axis of collimation was shifted by  $4^\circ$  from the geometric axis of the hole, assuming a uniform source. Using the transmission value together with the ratio of open area to total area of the disk, one gets a value of 0.74% for the transmission of the collimator disk. Thus, 1.48% of the fission events should give rise to a fragment which is recorded in the fission counter.

A  $100\text{-}\mu\text{gm/cm}^2$  gold foil covering the collimator disk served as a positive boundary to the sensitive volume of the fission counter so only fragments passing through the gold foil were recorded. The active volume of the counter was viewed by an RCA 6810-A photomultiplier tube, the face of which formed one end of the gas scintillation chamber. The face of the photomultiplier

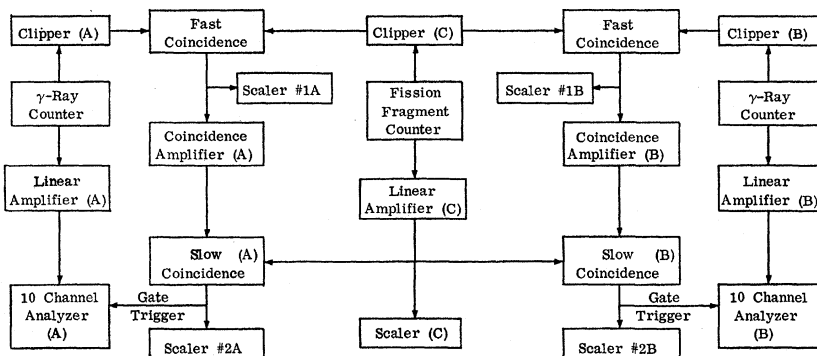


FIG. 3. Block diagram of electronic equipment.

was coated with diphenylstilbene to a thickness of approximately 100 Å. The counter gas was krypton which was purified in a chamber filled with hot metallic sodium-magnesium chips.

### Electronic Equipment

A block diagram of the electronic equipment used in this experiment is shown in Fig. 3. The two  $\gamma$ -ray counters utilized 1½-in. by 2-in. NaI(Tl) scintillation crystals and RCA 6810-A photomultiplier tubes. The photomultipliers of both the fission and  $\gamma$ -ray counters were operated into a pulse clipper and line driver which inverted and shaped the pulses and put them on a line terminated at the input end. At the other end of the line, the pulses were clipped by a shorted line and fed into a biased diode which determined whether a coincidence had occurred. A signal was also taken from the tenth dynode of each photomultiplier and amplified through a linear, delay-line-clipped pulse amplifier. Pulses from the linear channel of each  $\gamma$ -ray counter were analyzed by a 10-channel pulse-height analyzer. The linear channel from the fission fragment counter was fed into a scaler which counted the total number of fissions occurring. This channel was also used as one input to the slow coincidence unit, the other input being the fast coincidence output. The slow coincidence unit provided a reliable gating signal for the pulse-height analyzer and served to minimize the effect of noise from the fast coincidence amplifier. The electronic equipment was subjected to several checks for consistency of operation during periods when data were being collected. The fission rate and the fast and slow coincidence rates were monitored continuously. Measurements of the  $\gamma$  intensity at  $\theta=60^\circ$  were repeated at least three times during each data-taking period, and all data taken during the period were rejected if the measurements at  $\theta=60^\circ$  were not consistent. This check guarded against changes in the over-all sensitivity of the system. Some changes in sensitivity were found to occur as a result of photomultiplier fatigue. This problem was solved by reducing the reactor power level. Also, the counter response as a function of time delay was checked at a few points each day prior to recording data.

### EXPERIMENTAL RESULTS AND DISCUSSION

The data presented in Fig. 4 indicate that a small, but definite,  $\gamma$ -ray fission fragment directional correlation does exist. Since the probability of emission of a photon by an excited nucleus generally depends on the angle between the nuclear spin axis and the direction of emission, the experimental data indicate that a relationship exists between the nuclear spin axis and the direction of fragment motion, subsequently referred to as the fission axis. Thus, the fission configuration appears to influence the orientation, and most likely, the magnitude of the nuclear spin of the fragments. Assuming that fission fragments, after the emission of neutrons, decay toward the ground state by dipole radiations, the observed  $\gamma$ -ray correlation indicates a net polarization of the fragment angular momentum along the fission axis. On the other hand, if the observed  $\gamma$ -ray anisotropy is the result of predominantly quadrupole radiation, a net polarization of the angular momentum at  $90^\circ$  to the fission axis is indicated. The data points displayed in Fig. 4 have been analyzed to ascertain the most probable average values for the magnitude and orientation of the fragment angular momentum. It should be understood that the results of this analysis apply to fragment nuclei which have on the average already undergone the emission of 1.23, 1.22, and 1.45 neutrons per fragment of  $U^{233}$ ,  $U^{235}$ , and  $Pu^{239}$ , respectively.

It was assumed that the experimentally observed  $\gamma$ -ray distribution could be considered as a combination of three components, one of which was emitted isotropically, one having the shape of  $\gamma$  rays resulting from dipole transitions, and the other having the shape of  $\gamma$  rays resulting from quadrupole transitions. Thus, the data were fitted to the function

$$a + b\omega_1(\theta, J, \alpha) + c\omega_2(\theta, J, \alpha) \quad (1)$$

in which  $\omega_1$  and  $\omega_2$  represent the  $\gamma$ -ray intensities at the angle  $\theta$  resulting from dipole and quadrupole transitions, respectively.<sup>3</sup> The parameter  $J$  is the initial angular momentum of the emitting nucleus, while  $\alpha$  is a parameter which specifies the orientation of the initial angular

<sup>3</sup> *Beta- and Gamma-Ray Spectroscopy*, edited by Kai Siegbahn (Interscience Publishers, Inc., New York, 1955), p. 616.

momentum through the relation

$$a(m_i) = [(2\pi)^{1/2} J \alpha]^{-1} \exp[-m_i^2/2(J\alpha)^2]. \quad (2)$$

Thus  $\alpha$  enters into the expression for  $\omega(\theta)$  through its dependence on  $a(m_i)$ . The assumption of this normal distribution with mean value zero and variance of  $(J\alpha)^2$  for the population of angular momentum states is justified by a central limit theorem, if the following conditions are met<sup>4</sup>: (1) All the elements of  $X_k$  are independent. (2) The elements of any sequence of  $X_k$ 's are identically distributed. (3) The variance of any sequence of  $X_k$ 's is finite. The  $X_k$ 's are elements of a sequence of random variables defined on the orientation of nuclear angular momentum vectors. The spin state of each fragment pair is independent of the state of each other pair, although the two fragments from any one fission event are not independent. It was experimentally impossible, however, to observe a  $\gamma$  ray from both fragments of a fission event. Since the experimental observations are independent for all fragments, the probability of detecting  $\gamma$  rays from both fragment  $A$  and fragment  $B$  of a single fission event is the conditional probability  $P(A|B)$ , but because of independence,  $P(A|B) = P(A)P(B)$ . In this experiment  $P(A) \approx P(B) \approx 10^{-3}$  so the detection of two  $\gamma$  rays from a single fission was very rare. When it does occur, the two  $\gamma$  rays are combined, resulting in a fictitious, high-energy  $\gamma$  ray. Thus, each observation may be considered independent and condition (1) is satisfied. All sequences in  $X_k$  can be assumed to have the same distribution because they are the result of an arbitrary sampling of a random variable whose distribution does not change with time. Condition (3) is satisfied as a result of the boundedness of the magnitude of the angular momentum vector on which the random variable is defined.

Equation (1) was used to fit  $\gamma$ -ray distributions calculated using expression (2) to the experimental data. The functions  $\omega_1(\theta)$  and  $\omega_2(\theta)$  were first calculated for several different values of the parameters  $J$  and  $\alpha$ . A least-squares fit of the data from each of the fissioning nuclides was then calculated using all of the previously calculated functions  $\omega_1(\theta)$  and  $\omega_2(\theta)$  in turn. Thus for each set of values of the parameters  $J$  and  $\alpha$ , the corresponding  $\gamma$ -ray distribution was fitted to the data by adjusting the coefficients  $a$ ,  $b$ , and  $c$  of Eq. (1), and a

TABLE I. Summary of fission  $\gamma$ -ray data analysis.

Nuclide	Relative quality of fit <sup>a</sup>	Anisotropy	$J$	$\alpha$	$a^b$	$b$	$c$
Pu <sup>239</sup>	1.967	0.15 ± 0.02	6 ± 1	0.300	1.00	≤ 0.01	0.193 ± 0.017
U <sup>235</sup>	4.762	0.12 ± 0.02	7 ± 2	0.325	1.00	≤ 0.01	0.130 ± 0.020
U <sup>235</sup>	3.489	0.13 ± 0.02	8 ± 2	0.363	1.00	≤ 0.01	0.157 ± 0.020

<sup>a</sup> The numbers in this column are proportional to the sum of squares of deviations for the least-squares fit of Eq. (1) to the experimental data points.

<sup>b</sup> A condition of the least-squares fit was  $a = 1$ .

<sup>4</sup> M. Loève, *Probability Theory* (D. Van Nostrand Company, Inc., Princeton, New Jersey, 1960), 2nd ed., p. 295.

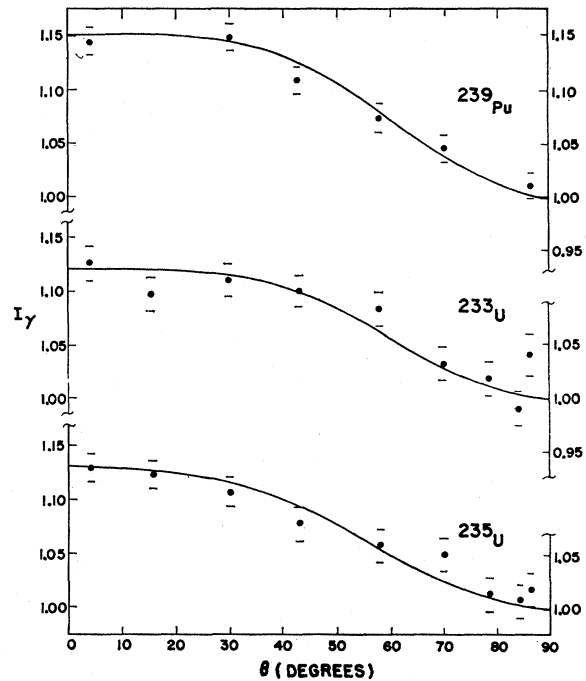


FIG. 4. Measured relative number of  $\gamma$  rays having energy greater than 250 keV as a function of the angle to the fragment direction. The solid curves are the results of a least-squares fit of  $a + b\omega_1(\theta) + c\omega_2(\theta)$  to the data points.  $\omega_1(\theta)$  and  $\omega_2(\theta)$  are the calculated dipole and quadrupole  $\gamma$ -ray distributions from nuclei whose angular momentum exhibits a normal distribution in the population of magnetic substates quantized along the fission axis. The variance of the normal distribution and the total angular momentum were allowed to vary in addition to the coefficients  $a$ ,  $b$ , and  $c$ , to minimize the sum of squares of the deviations.

measure of the goodness of the fit was obtained in the value of the sum of the squares of the deviations. These numbers which characterized the fits form a sequence, the nature of which can be used to determine whether this approach may be useful in studying fragment angular momentum. The results of this process show that for each individual value of  $J$  some specific value of the variance  $(J\alpha)^2$  is selected. This selected value, however, is not independent of  $J$ , but shifts to lower or higher values as  $J$  assumes lower or higher values. If, from the sequence of values for the sum of the squares of the deviations for each value of  $J$ , the minimum value is chosen and these are used to form another sequence indexed by  $J$ , the minimum of this last sequence selects a  $J$ , and therefore, a  $(J\alpha)^2$  which best fits the data. It should be emphasized that, while the indication is that the sequence from which  $J$  is selected has a minimum value and increases monotonically from this value for both larger and smaller values of  $J$ , the minimum is rather broad and because of the rather extensive calculations involved in arriving at each member of the sequence, it has not been extended beyond five elements.

The results of this method of analyzing the data fits are summarized in Table I. Gamma-ray data from the

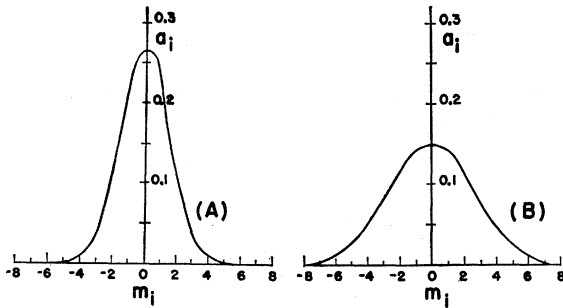


Fig. 5. Relative population of angular momentum substates quantized along the fission axis as predicted by the experimental  $\gamma$ -ray data for thermal neutron fission of  $\text{Pu}^{239}$  (A) and  $\text{U}^{235}$  (B).

thermal neutron fission of  $\text{Pu}^{239}$ ,  $\text{U}^{233}$ , and  $\text{U}^{235}$  indicate the existence of 6 to 8 units of angular momentum per fragment, on the average. This analysis of the experimental data results in an uncertainty of about 2 units in the predicted value of  $J$ . As a result, it cannot be said that this analysis predicts a different magnitude of angular momentum for the fission fragments of  $\text{Pu}^{239}$  than it does for  $\text{U}^{235}$ . This analysis also predicts that the angular momentum is preferentially oriented about an angle of  $90^\circ$  to the direction of motion of the fragment. Assuming that the angular momentum is normally distributed about this direction, the relative population of substates quantized along the axis of motion is represented in Fig. 5(A) for  $\text{Pu}^{239}$ , and Fig. 5(B) for  $\text{U}^{235}$ . Figure 5(A) is a plot of Eq. (1) for  $\alpha=0.300$ , and Fig. 5(B) is the same function for  $\alpha=0.363$ . This change in  $\alpha$  is about two times the maximum expected error so there is a strong indication that the angular momentum of  $\text{Pu}^{239}$  fragments is more strongly polarized than that of  $\text{U}^{235}$ . The best fits of the function (1) to the  $\text{Pu}^{239}$  and  $\text{U}^{233}$  data gave a value very near to zero for the coefficient  $b$ , and values of 0.193 and 0.130, respectively, for  $c$ , if  $a$  is fixed at one. Thus, these data indicate that there is no appreciable  $\gamma$ -ray anisotropy arising from dipole emission from these two nuclides. In the case of  $\text{U}^{235}$ , the coefficient  $b$  definitely tended to be negative, so that the fit was rerun with the value of all coefficients constrained to remain positive. Under this condition the calculated values of the coefficients were  $a=1$ ,  $b<0.01$ , and  $c=0.157$  and the sum of the squares of the deviations increased slightly. It can be seen from Table I that the sum of the squares of the deviations is smaller for the  $\text{U}^{235}$  data than the  $\text{U}^{233}$  data in spite of this added restraint.

The  $\gamma$ -ray anisotropy  $A = [I(0) - I(90)]/I(90)$  varies from 0.12 for  $\text{U}^{233}$  to 0.15 for  $\text{Pu}^{239}$ , a difference which is insignificant considering the statistical errors on the data which are reflected in a standard deviation of 0.02 for the value of  $A$  for all three nuclei. This value of 12% to 15% is lower than previously reported values. The higher values previously reported may have resulted from the counting of neutrons in the  $\gamma$  counters. Special efforts previously discussed diminished that difficulty

in this experiment. It is estimated that the effect of high-energy fission neutrons could be to increase the measured value of the  $\gamma$ -ray anisotropy by no more than 0.005. Since the correction for this effect would be relatively uncertain although quite small it has not been applied to the data, but is included in the error of  $\pm 0.02$  on  $A$ .

The influence of the ground-state angular momentum of the fissioning nucleus on the fragment angular momentum should have a slight effect on the measured  $\gamma$ -ray anisotropy. To determine the magnitude of this effect, it has been assumed that the 6 to 8 units of fragment angular momentum indicated by the data lie in the plane at  $90^\circ$  to the fragment motion. To this has been added a second angular momentum component which is randomly oriented and has a magnitude representative of the fissioning nucleus. Using the resulting angular momentum condition, the anisotropy of the emitted quadrupole  $\gamma$  rays has been calculated. The results of this calculation show that if the average unoriented angular momentum of fission fragments is half that of the ground state of the fissioning nucleus, the measured  $\gamma$ -ray anisotropy should decrease from 15% to 14% in going from  $\text{Pu}^{239}$  with spin  $\frac{1}{2}$  to  $\text{U}^{235}$  with spin  $\frac{7}{2}$ . Even if it is assumed that the average residual fragment angular momentum is equal to the ground-state spin of the fissioning nucleus, the  $\gamma$ -ray anisotropy for  $\text{U}^{235}$  is still calculated to be 12.5% compared to a value of 15% for  $\text{Pu}^{239}$ . The experimental results are consistent with this prediction. However, the magnitude of the predicted change in  $A$  between  $\text{Pu}^{239}$  and  $\text{U}^{235}$  fission is too small to be measured reliably by this experiment.

The rather rudimentary energy analysis of the observed  $\gamma$  rays which was possible with two 10-channel pulse-height analyzers did not reveal any  $\gamma$ -energy regions exhibiting pronounced differences in anisotropy. The results indicated that  $\gamma$  rays in the interval between 0.250 and 1.25 MeV were preferentially emitted along the axis of fragment motion. There was some indication, however, that a slightly higher degree of anisotropy existed for  $\gamma$  rays in the energy range from 0.400 to 0.700 MeV.

The over-all picture is one in which the fragments resulting from thermal neutron fission of  $\text{Pu}^{239}$ ,  $\text{U}^{233}$ , and  $\text{U}^{235}$  appear to have 6 to 8 units of angular momentum oriented preferentially about  $90^\circ$  to the fission axis after the emission of fission neutrons. Since fragment angular momentum induced by electrostatic forces between the fragments would be oriented in a manner consistent with these experimental results, a calculation to estimate the magnitude of angular momentum thus induced was performed. Strutinskii's<sup>5</sup> estimation of induced angular momentum was so high as to appear quite inconsistent with the results of this experiment.

<sup>5</sup> V. M. Strutinskii, Zh. Eksperim. i Teor. Fiz. **37**, 861 (1959) [translation: Soviet Phys.—JETP **10**, 613 (1960)].

## DISCUSSION OF TORQUE CALCULATION

In considering the question of the induced angular momentum of fission fragments, one might ask only whether some net average, nonsymmetric distortion of the fragment does, in fact, persist for times as long as  $10^{-21}$  sec. If this is the case, the Coulomb repulsive force will be such that some portion of the Coulomb energy of the fragments will appear as rotational kinetic energy. While the sole assumption of nonsymmetric nuclear distortion indicates an induced angular momentum in the distorted nucleus, the calculations herein described attempt to estimate the magnitude of the induced angular momentum on the basis of reasonable assumptions concerning the fission configuration, and show that the results are very sensitive to several parameters of the problem.

This calculation was set up as though the heavy fission fragment were spherical and the light fragment possessed a prolate spheroidal distortion. This idealized representation enables one to write an exact expression for the force between the two charges. By a proper choice of point charges, the same expression can be used to approximate the electrostatic forces between two fission fragments, both of which have spheroidal distortions. Prompt neutron measurements from fission fragments do, however, indicate that the average distortional energy of the light fragment is, in fact, larger than that of the heavy fragment which lies in the closed-shell region. The components of force between a uniformly charged sphere and spheroid, if the sphere is represented by a point charge at its origin, are given by<sup>6</sup>

$$\frac{F_x}{x} = \frac{F_y}{y} = 2\pi\sigma q \left(\frac{1}{\epsilon^3}\right) \left\{ \frac{a\epsilon}{(a^2+K)^{1/2}} \left(1 - \epsilon^2 + \frac{a^2\epsilon^2}{a^2+K}\right)^{1/2} - (1 - \epsilon^2) \ln \left[ \frac{a\epsilon}{[(1 - \epsilon^2)(a^2+K)]^{1/2}} + \left(1 + \frac{a^2\epsilon^2}{(1 - \epsilon^2)(a^2+K)}\right)^{1/2} \right] \right\} \quad (3)$$

and

$$\frac{F_z}{z} = 2\pi\sigma q \left(\frac{1 - \epsilon^2}{\epsilon^3}\right) \times \left[ \frac{-2c\epsilon}{(c^2+K)^{1/2}} + \ln \frac{1 + c\epsilon/(c^2+K)^{1/2}}{1 - c\epsilon/(c^2+K)^{1/2}} \right], \quad (4)$$

in which

$$K = \frac{1}{2}c^2\epsilon^2 + \frac{1}{2}r^2 - c^2 + \frac{1}{2}(c^2\epsilon^2 + r^2 - 4c^2\epsilon^2r^2 \cos^2\Psi)^{1/2} \quad (5)$$

is the real positive root of the equation of the spheroid

$$\frac{x^2}{a^2+K} + \frac{y^2}{a^2+K} + \frac{z^2}{c^2+K} = 1. \quad (6)$$

The semiminor and semimajor axes of the spheroid are given by  $a$  and  $c$ , respectively;  $\Psi_0$  represents the angle between the major axis of the spheroid and a line joining the centers of charge of the two fragments, and  $\epsilon = (1 - a^2/c^2)^{1/2}$  defines the shape of the spheroid. The quantity  $\sigma$  of Eqs. (3) and (4) represents the charge density of the spheroidal body and  $q$  represents the total charge of the spherical body which can be assumed to be a point charge. For this calculation  $\sigma$  is the charge density of a fission fragment nucleus while  $q$  is the charge of the complementary fragment. The  $\Psi$  which appears in the expression for  $K$  is measured between the major axis of the spheroid and the line joining the centers of charge of the two bodies. The initial value of  $\Psi$  represented by  $\Psi_0$  is discussed below.  $R$  is the distance between the center of charge of the two bodies and its initial value is  $R_0$ . In determining  $R_0$  it is assumed that the two charged bodies are in a static condition so that the total kinetic energy of fission appropriate to the selected fragment mass ratio appears as electrostatic energy. For the sphere-spheroid configuration, a good value of  $R_0$  results from evaluating

$$E_{ke} = qq' \frac{1}{R_0} \left( 1 + \frac{3c^2\epsilon^2}{15R_0^2} + \frac{3c^4\epsilon^4}{35R_0^4} + \dots \right), \quad (7)$$

for  $R_0$  where  $q$  and  $q'$  are the net charges on the two bodies and  $E_{ke}$  is the total fragment kinetic energy. The time  $t$  also is measured relative to this static condition of the system so that at  $t=0$ ,  $R=R_0$  and  $\Psi=\Psi_0$ . From these initial conditions the configuration of the system evolves in time under the influence of electrostatic and inertial forces. The coordinates of the center of charge of the sphere are given by  $x$ ,  $y$ , and  $z$ , also  $r = (x^2 + y^2 + z^2)^{1/2}$ . In this coordinate system the spheroid is fixed with its center of charge at the origin and its major axis along the  $z$  axis. The choice of this coordinate system serves to simplify the force expressions.  $F_x$ ,  $F_y$ , and  $F_z$  are the components of the electrostatic force between the two bodies. An IBM 704 was used to evaluate the function  $\int (F \times R) dt$ . Unfortunately, the interesting region of the domain of this function is not completely known. Appropriate ranges for the values of  $q$ ,  $R_0$ , and  $t$  can be determined, but  $\Psi_0$ , the initial orientation, and  $\epsilon$ , the degree of distortion of the spheroid, can only be estimated within rather wide limits. For this reason the mapping has been carried out for several points in the product space of  $\Psi_0$  and  $\epsilon$ . This space can be thought of as a hyperplane in the space of  $(R_0, t, \Psi_0, \epsilon)$ . Figure 6 shows the product space of  $\Psi_0$  and  $\epsilon$  with contour lines representing the locus of some points for which  $\int (F \times R) dt$ , the induced angular momentum, is con-

<sup>6</sup> F. R. Moulton, *Celestial Mechanics* (The Macmillan Company, New York, 1953), 2nd revised ed., p. 127, ff.

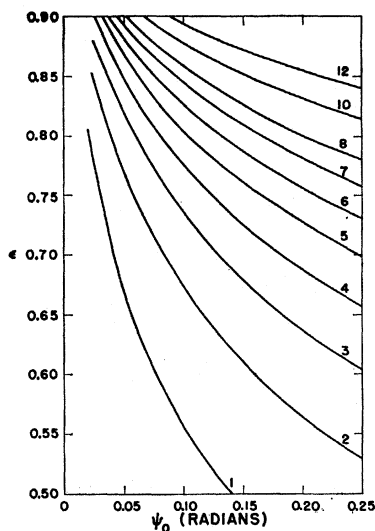


FIG. 6. Calculated fragment angular momentum in units of  $\hbar$ . The lines represent the locus of points in  $\psi_0$  and  $\epsilon$  product space which are mapped by the torque calculation into the real numbers with which each line is labeled.

stant. The range of nuclear distortions covered by the calculation extends from  $\epsilon=0.5$ , corresponding to distortions only a little larger than those occurring in the ground states of some intermediate mass nuclei, up to  $\epsilon=0.9$ . The value of 0.9 for  $\epsilon$  is estimated to correspond to an energy of distortion of about 18 MeV per fragment nucleus,<sup>7</sup> and a ratio of major to minor axis of a little more than 2 (Fig. 7). While this value is small compared to elongations of fissioning nuclei which are sometimes assumed to be as great as ten, it appears that for nuclei in the fragment mass range that energy considerations will not allow greater distortions to exist long enough to be significant.

The nuclear moment of inertia  $\mathcal{L}$  is not well known for nuclei with excitation energies similar to those of fission fragments at the scission point. Experimental values of  $0.27\mathcal{L}_{\text{rig}} \leq \mathcal{L} \leq 0.48\mathcal{L}_{\text{rig}}$  have been reported for nuclei in comparable mass and excitation regions.<sup>8</sup>  $\mathcal{L}_{\text{rig}}$  represents the moment of inertia of a rigid spheroid about a minor axis. The values of  $J$  shown in Fig. 6 resulted from using  $\mathcal{L}=0.5\mathcal{L}_{\text{rig}}$ . In Fig. 8 the variation

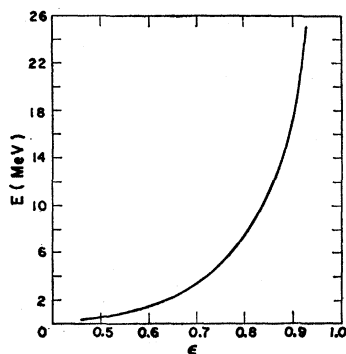


FIG. 7. Approximate energy associated with a prolate spheroidal distortion for a fragment nucleus of mass 96.

<sup>7</sup> W. J. Swiatecki, Proc. Intern. Conf. Peaceful Uses of At. Energy, Geneva, 1958 **15**, 248 (1958).

<sup>8</sup> J. L. Need, Phys. Rev. **129**, 1302 (1963).

of the calculated  $J$  resulting from changes in  $\mathcal{L}$  is shown for four points in the  $(\Psi_0, \epsilon)$  product space. The calculated values of  $J$  are not strongly dependent upon the moment of inertia for  $\mathcal{L} \geq 0.4\mathcal{L}_{\text{rig}}$ .

Provisions were made for the quantization of the calculated induced angular momentum. The effect of the quantization conditions, however, was of negligible magnitude for calculated values greater than  $3\hbar$ .

The range of  $\Psi_0$  considered was made large enough to display characteristics of the induced angular momentum as a function of  $\Psi_0$ , and to include the value of  $\Psi_0$  which one might assume from the following argument to be a reasonable average value. If an axis of rotational symmetry actually does exist throughout the entire fission process, as is often assumed, the force expressions used in this calculation will always give zero torque. Strict rotational symmetry of a fissioning nucleus would not be expected in practice, however, for even though the nucleus moves toward the saddle point, up a potential energy valley whose minimum lies along a symmetric distortion coordinate, it is energetically possible

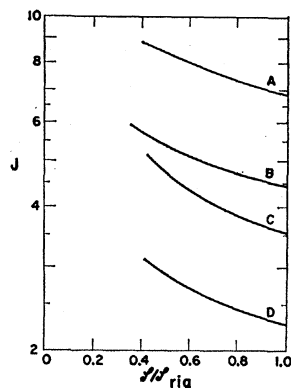


FIG. 8. Variation in the calculated fragment angular momentum resulting from a change in the assumed value for the nuclear moment of inertia. The lines labeled A, B, C, and D represent the change in the mapped value of the points at  $(0.1, 0.85)$ ,  $(0.1, 0.80)$ ,  $(0.05, 0.85)$ , and  $(0.05, 0.80)$ , respectively, in the  $(\psi_0, \epsilon)$  space of Fig. 6.

to depart from the potential minimum via an asymmetric distortion coordinate. Many degrees of freedom in asymmetric oscillations on the potential surface will exist for nuclei near the saddle point. By choosing a model with an oscillatory mode in a coordinate which is correlated with the angle  $\Psi$  of our torque calculation, an expectation value for that coordinate can be calculated which will represent a statistical average for  $\Psi$ .

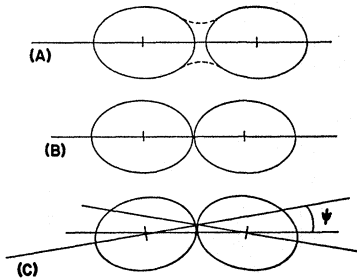
Assuming that nuclei pass through the saddle point region slowly compared to the period of oscillation in  $\Psi$ , this statistical average will hold approximately at the scission point if the scission point and saddle point configurations are not too dissimilar. The value of  $\Psi$  should be chosen as the statistical average value of  $\Psi$  at the scission point if the torque calculation is to lead to an average induced fragment angular momentum. The two-spheroid model shown in Fig. 9(B) is used to estimate  $\Psi_0$ . Cohen and Swiatecki<sup>9</sup> have shown that for values of  $x = (\text{charge})^2 / (\text{surface tension} \times \text{volume} \times 10)$

<sup>9</sup> S. Cohen and W. J. Swiatecki, Ann. Phys. (N. Y.) **22**, 406 (1963).

$\leq 0.7$ , two nearly tangent spheroids connected by a neck of length  $(0.2R_0)(4\pi/3)^{1/3}$  is a good approximation [Fig. 9(A)] to the saddle point configuration. Since nuclei having  $x \sim 0.7$  are being considered, the simple two-tangent spheroid model appears to be applicable. As a result of this simplified model the saddle point coincides with the scission point, so the average saddle point value of  $\Psi$  can be used directly for  $\Psi_0$ .

The usefulness of the two-spheroid saddle point model of Fig. 9(B) has been demonstrated by Nix<sup>10</sup> who used it to calculate the most probable fragment kinetic energies and the width of kinetic-energy distributions. The results of his calculations are in reasonable agreement with experimental results. While the calculations of Nix utilized a configuration having an axis of rotation [Fig. 9(B)] on which the spheroids are tangent at their vertex points, if the constraint of rotational symmetry is not imposed on the model, configurations of the type shown in Fig. 9(C) must be considered. A Hamiltonian for small amplitude oscillations in  $\Psi$  about  $\Psi=0$  can be written as  $H = \frac{1}{2}\mathcal{L}_1\dot{\Psi}^2 + \frac{1}{2}K\Psi^2$ , in which  $\mathcal{L}_1$  is the effective moment of inertia for the

FIG. 9. (A) Approximate saddle point configuration as given by Cohen and Swiatecki. (B) Two-tangent-spheroid saddle point model. (C) Two-tangent-spheroid saddle point model not constrained to an axis of rotational symmetry.

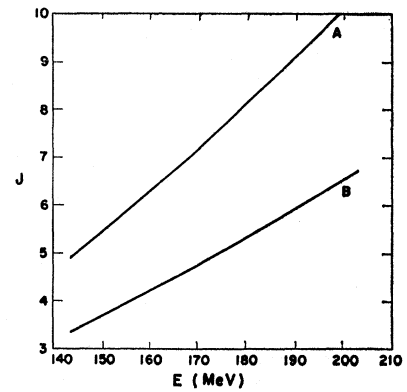


spheroid about the vertex and  $K$  is the force constant acting between the centers of charge of the spheroids. This is the harmonic oscillator Hamiltonian so the zero-point energy harmonic oscillator wave function was used to calculate an expectation value of  $|\Psi|$ . This was found to be  $\langle |\Psi| \rangle \approx 0.06$ . For this calculation, the charge and mass distribution among the fragments and the effective moment of inertia enter only as the fourth root, so the value of  $\langle |\Psi| \rangle$  is quite insensitive to these quantities. The expectation of this coordinate at the scission point is just the value required for the calculation parameter  $\Psi_0$ . It appears, therefore, that  $0.05 \leq \Psi_0 \leq 0.1$  is a reasonable estimate for  $\Psi_0$  in the torque calculation.

The contours of Fig. 7 for constant values of  $J$  show the results of the torque calculation for a range of values of  $\Psi_0$  and  $\epsilon$ . The following values were used for the other variables of the problem: The initial separation of the centers of the two bodies was  $1.90 \times 10^{-12}$  cm. The charge and mass ratios were 1.19 and 1.30, respectively, and the total charge and mass of the two bodies

<sup>10</sup> L. R. Nix, Lawrence Radiation Laboratory Report UCRL-10695, April 1963 (unpublished).

FIG. 10. Calculated angular momentum as a function of the total kinetic energy of the fragments. The functional relationship displayed here is established through the variations of the calculated angular momentum and the electrostatic energy of the fragments with the parameter  $R_0$ . The curve A is for  $\psi_0=0.1$ ,  $\epsilon=0.85$  and the curve B is for  $\psi_0=0.1$ ,  $\epsilon=0.80$ .



corresponded to that of the  $U^{236}$  nucleus. The nuclear moment of inertia used here was one-half the moment of a rigid spheroid about a minor axis. The low-mass body was assumed to possess the spheroidal distortion.

A calculation whose results are applicable to a fissioning nucleus must allow for distortions to exist in both fragments, and for the nature and magnitude of the distortions to vary with time. Because of the difficulty of the dynamical problem, some highly simplified approximations have been investigated which gave an indication of the results to be expected from a more rigorous treatment of the problem.

To determine the gross change in the calculated torque arising from the second charge having a spheroidal distortion in contrast to being spherical, a spheroidal charge distribution was approximated by a series of point charges. The magnitude and position of the point charges were adjusted so that the total electrostatic energy between the two bodies was similar to the total kinetic energy of uranium fission. Also, the equal potential surface which corresponded to the spherical nuclear surface when the total nuclear charge was assumed to be at the center point of the sphere, was made to approximate a spheroid of  $\epsilon \approx 0.77$  which enclosed the same volume as the sphere. While this is not a particularly good approximation to a spheroid, the electrostatic energy between a point charge and a spheroid approximated by two like charges differs by only 2% from that between a point charge and a uniform spheroidal charge distribution having an  $\epsilon$  equal to that approximated by the two-charge configuration.

The results indicate that the calculated angular momentum would be expected to increase by 10% for the case of two equally distorted bodies, assuming that the inertial properties of both spheroids were similar to those of the spheroid discussed previously.

Figure 11 has been prepared to show how the calculated angular momentum varies with the total fragment kinetic energy if the fragment distortion is unchanged. The energy used in Fig. 11 is the electrostatic energy between two uniformly charged prolate spheroids. From Fig. 10 it can be seen that the induced angular momen-



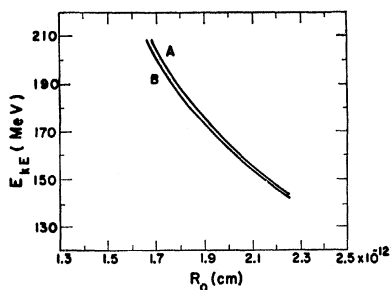


FIG. 11. The electrostatic energy versus separation of centers of charge for two uniformly charged prolate spheroids whose major axes are colinear and whose eccentricities are given by  $\epsilon=0.77$  and  $0.85$  (curve A) and  $\epsilon=0.77$  and  $0.80$  (curve B). This energy-distance relationship was used to prepare Fig. 10.

tum of fission fragments is calculated to be appreciably higher if the total fragment kinetic energy is high. Thus, fission which results in a heavy fragment in the 130–135 mass region and an average total kinetic energy of about 170 MeV, might be expected to have 50% more induced angular momentum than nearly symmetric fission for which the average total kinetic energy decreases to about 140 MeV. Figure 10 shows the results obtained by representing one fragment by a uniformly charged prolate spheroid, and the other by two similar point charges placed on the major axis of the spheroid which they simulate. The two similar point charges were separated by a distance of  $7.52 \times 10^{-13}$  cm, which results in their representing a spheroid characterized by  $\epsilon \approx 0.77$ . Values of  $R_0$ , the separation between centers of the charge configurations representing the two fragments, were then calculated which corresponded to several different total fragment energies. Figure 11 shows the  $R_0$  versus electrostatic energy relationship for two values of  $\epsilon$  for the uniformly charged spheroid. Since the assumed value of  $R_0$  which gives rise to the proper observed fragment kinetic energy depends in turn on the nuclear shape assumed, slight adjustments may be required in this parameter. For this reason, Fig. 12 shows how the calculated angular momentum is expected to vary with  $R_0$  if the other parameters are held constant. If the average fragment kinetic energy for thermal neutron fission of uranium is taken to be 167 MeV, the calculated average induced angular

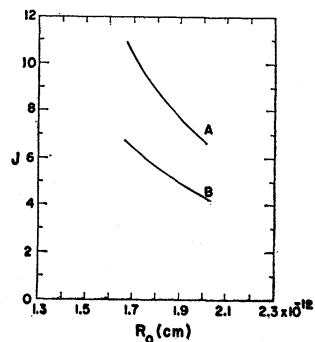


FIG. 12. Variation of calculated angular momentum of a spheroid with  $R_0$  (the charge separation) used in the preparation of Fig. 10. Curve A results from  $\psi_0=0.1$ ,  $\epsilon=0.85$  and curve B from  $\psi_0=0.1$ ,  $\epsilon=0.80$ .

momentum is seen to lie between  $4.5$  and  $7\hbar$  depending on the effective value of  $\epsilon$ .

The rotational kinetic energy commensurate with the induced angular momentum  $J$  is shown in Fig. 13 for an average light fragment (A) and an average heavy fragment (B). Since  $\gamma$ -ray transitions from rotational states must be slow compared to neutron emission, the fragment nuclei undergoing rotational transitions will have an average internal excitation energy equal to or less than about 2 MeV.<sup>11,12</sup> Thus no large distortions of the fragment nuclei can occur after neutrons have been emitted. As a result the moments of inertia of fragment nuclei undergoing rotational transitions will be comparable to those of medium mass nuclei having modest excitation energies.<sup>13</sup> For this estimate of rotational energy  $E_r = (\hbar^2/2\mathcal{I})[J(J+1)]$ , the moment of inertia  $\mathcal{I}$  was taken as  $0.5(\frac{2}{3}MR^2)$  or half the moment of the rigid spherical nucleus. The rotational energy corresponding to the calculated value of  $6\hbar$  is then in

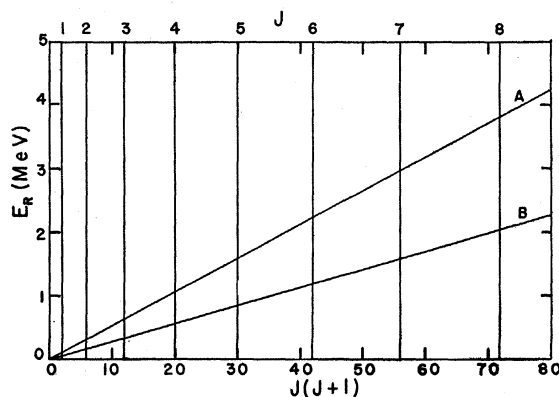


FIG. 13. Rotational kinetic energy versus angular momentum for average light fragments (A) and average heavy fragments (B) at a time sufficiently long after scission that large fragment distortion no longer exists. For this figure the nuclear moment of inertia was assumed to be one-half that of a rigid sphere.

the neighborhood of 1.2 MeV per heavy fragment and 2.25 MeV per light fragment. The lifetimes of these energy states would be expected to be sufficiently long so that the problem of neutron and  $\gamma$ -ray emission from an excited fragment nucleus could not be treated simply by the statistical method. The  $\gamma$  rays from transitions between rotational states could possibly enhance the total  $\gamma$ -ray energy by 3.5 MeV per fission over that calculated by the statistical method.<sup>11</sup>

It is further predicted that the energy of the quadrupole transitions occurring below the  $J=6\hbar$  rotation state would range from 1.25 to 0.15 MeV. It is thus understandable that the energy dependence of the  $\gamma$ -ray correlation might change very slowly over the energy range 0.25 to 1.25 MeV in which  $\gamma$  rays were analyzed

<sup>11</sup> R. B. Leachman, Phys. Rev. **101**, 1005 (1956).

<sup>12</sup> R. B. Leachman and C. S. Kazek, Jr., Phys. Rev. **105**, 1511 (1957).

<sup>13</sup> J. J. Griffin and M. Rich, Phys. Rev. **118**, 850 (1960).

in this experiment and would, therefore, have been difficult to detect. Had the  $\gamma$  rays been energy analyzed in the region of 1.5 MeV or above, the directionally correlated  $\gamma$  rays from rotational transitions should not have been present, and no directional correlation would have been observed in this  $\gamma$ -ray energy region.

A most important and difficult aspect of the problem is to determine how the shape of the fragment changes in time. To avoid using a distortion magnitude which is almost surely an incorrect function of time, all the calculated results shown are for  $\epsilon(t) = \text{constant}$ . The remaining problem then is to determine an average effective value for the nuclear distortions which is applicable for times up to  $10^{-21}$  sec. The distortions existing at scission are estimated from energy considerations to be represented by  $\epsilon \approx 0.86$ , or perhaps slightly larger, but probably not larger than  $\epsilon = 0.90$ .

The manner in which a fission fragment departs from its scission point shape has not been studied in detail, but there is some indication that it may not pass through a spherical shape. The light and heavy fragments will contain in the neighborhood of 56 and 88 neutrons, respectively. The neutrons which are outside of closed shells will tend to give rise to a nonspherical nuclear shape.<sup>14</sup> Under the influence of the large distortions present in the highly excited fission fragments the residual interaction between nucleons is greatly reduced which allows the polarizing effect of nucleons outside of closed shells to be more pronounced.<sup>15</sup> The observed systematic decrease in the energy of the first  $2+$  levels of even-even nuclei of  $38 \leq Z \leq 42$ , as pairs of neutrons are added, demonstrates a trend toward reduced rigidity for nuclei which are similar to the neutron-rich light fission fragments. For nuclei in the region of heavy fragments the excitation of the first  $2+$  state drops rapidly with increasing neutron number and remains at a nearly constant low value for  $90 \leq N \leq 110$ . Since both fragments are highly distorted and neutron rich, their shapes should be determined by potentials which according to the arguments of Alder *et al.*<sup>15</sup> are much broader than those of normal medium-mass nuclei.

If the oscillatory motion of a fragment after scission is relatively unaffected by its large distortion and shell structure, the initial motion will be determined by a potential similar to that shown in Fig. 7, which can be expressed as a function of a new coordinate  $q = c \times [1 - (1 - \epsilon^2)^{1/2}]$ . This coordinate is the difference between the semimajor axis and the semiminor axis of the spheroid. In this coordinate, the potential in which the nucleus will move is approximately parabolic, at least near the classical turning points. From this potential shape, the indication is that appreciable distortion should not be expected for more than

$(2-3) \times 10^{-21}$  sec after scission. For shorter times an average effective  $\epsilon$  of 0.8 to 0.85 might be expected.

### CONCLUSIONS

Results of this calculation of the torque on uniformly charged spheroidal bodies, designed to simulate fragment nuclei in the latter stages of nuclear fission, indicate that some induced angular momentum is to be expected. Using values which appear reasonable for the many parameters which enter into the angular momentum calculation results in a calculated average value of 5 to  $6\hbar$  per fragment. The fission fragment  $\gamma$ -ray correlation experiment shows that a 12 to 15% anisotropy exists for  $\gamma$  rays associated with thermal neutron fission of  $U^{233}$ ,  $U^{235}$ , and  $Pu^{239}$ . Analyses of the measured  $\gamma$ -ray distributions indicate that the anisotropy is due to quadrupole transitions of fragment nuclei which possess an average initial angular momentum of  $7 \pm 2\hbar$  which is oriented near a plane perpendicular to the fission axis. The study of some isomeric ratios in low and medium energy fission products<sup>16</sup> has led to estimates of 6 to 10 units of angular momentum per fragment. The fragment angular momentum deduced from the  $\gamma$ -ray measurements must be considered as an average over all fragment masses, while the results of shielded isomer ratio studies apply to one specific fragment mass. Fragments of mass 114 to 122, in keeping with their low total kinetic energy, would most likely have appreciably less induced angular momentum than the average. There should also be cases in which, due to nuclear shell effects, the fragment distortion is unusually small and results in little or no induced angular momentum in that particular nuclide. Both  $Cs^{134}$  and  $Te^{131}$  in which the high spin isomers are reported to be favored, are in a fragment mass region commensurate with an average total kinetic energy about 5% higher than that for all fragments. As a result, the calculation predicts an average induced angular momentum of 5.5 to 7 units for fragments in the mass range of these isotopes. The results of this calculation show that the presence of fragment angular momentum of a magnitude consistent with experimental results can arise from electrostatic forces between the fragments.

### ACKNOWLEDGMENTS

The help of Mrs. Marilyn Cowan and Mrs. Elizabeth Bowers in taking and analyzing the experimental data, and the valuable assistance of the members of the Los Alamos Water Boiler Group is gratefully acknowledged. My special thanks go to Dr. R. B. Leachman and Dr. J. J. Griffin for valuable discussions and suggestions, and to Miss Faye M. Lee for programming the machine calculations. It is also a pleasure to acknowledge the constant aid and support of Dr. R. L. Aamodt.

<sup>14</sup> J. Rainwater, Phys. Rev. **79**, 432 (1950).

<sup>15</sup> K. Alder, A. Bohr, T. Huus, B. Mottelson, and A. Winther, Rev. Mod. Phys. **28**, 432 (1956).

<sup>16</sup> H. Warhanek and R. Vandenbosch (private communication).

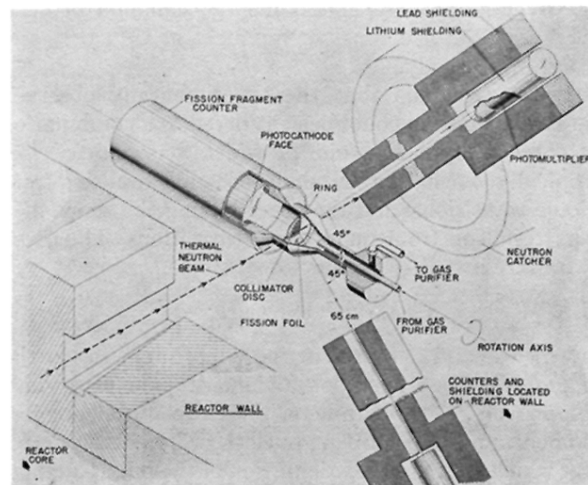


FIG. 1. Counter configuration used to measure fission fragment  $\gamma$ -ray correlation.